INDEPENDENT JOURNAL OF MANAGEMENT & PRODUCTION (IJM&P)
http://www.ijmp.jor.br *v. 11, n. 4, July - August 2020*
ISSN: 2236-269X
DOI: 10.14807/ijmp.v11i4.989

TRABECULAR PROSTHESES

Raffaella Aversa
Advanced Materials Lab, Department of Architecture and Industrial Design, Second University of Naples, Italy
E-mail: raffaella.aversa@unina2.it

Relly Victoria Virgil Petrescu
Bucharest Polytechnic University, Romania
E-mail: rvvpetrescu@gmail.com

Antonio Apicella
Advanced Materials Lab, Department of Architecture and Industrial Design, Second University of Naples, Italy
E-mail: antonio.apicella@unina2.it

Florian Ion Tiberiu Petrescu
IFToMM, Romania
E-mail: fitpetrescu@gmail.com

Submission: 1/23/2019
Revision: 2/27/2019
Accept: 9/19/2019

ABSTRACT

The complex biomechanics and morphology of the femur proximal epiphysis are presented. This specific region in the human femur is characterized by high flexibility compared to that of other primates, since evolved lighter and longer due to the human vertical position and more balanced loading. The nature and fine morphology of the femur head and its structural behavior have been investigated. Isotropic and orthotropic trabecular structures, which are not present in other primates, have been associated with compression and tension areas of the femur head. These isotropic/orthotropic trabecular morphologies and allocations govern the stress and strain distribution in the overall proximal femur region. Use of femur proper biofidel modeling while enabling the explanation of physiological stress distribution elucidates the critical mechanical role of the trabecular bone that should be accounted in the design of a new innovative more “biologic” prosthetic system.

Keywords: Trabecular lattice, Biomimetic, Trabecular prostheses.

ISSN: 2236-269X
DOI: 10.14807/ijmp.v11i4.989

1. INTRODUCTION

Trabecular bone stability depends not only on the amount of bone tissue but also on the three-dimensional orientation and the trabecular connection, which is summarized as trabecular micro-arhitectomy. In previous studies, we could demonstrate that in three-dimensional bone tissue, the relationship between trabecular plate and stems is reflected in the ratio of concave to convex surfaces of the bone model in two-dimensional bone sections. To quantify the relationship between these bone models, we developed a new histomorphometric parameter called the Trabecular Axis Model Factor (TBPf).

The basic idea is that the relationship between structures can be described by the relationship between convex and concave surfaces. A plurality of concave surfaces is a well-connected sponge, while a plurality of convex surfaces indicates a trabecular part poorly connected in two-dimensional sections. Using an automatic image analysis system, can measure the trabecular bone area (A1) and the perimeter (P1). The second measurement of these two parameters (now A2 and P2) is done after a trabecular expansion simulated on the screen. This dilation results in a characteristic change in bone area and perimeter depending on the ratio between convex and concave surfaces.

TBPf is defined as a difference between measurements 1 and 2: TBPf = (P1 - P2) / (A1 - A2). The first TBPf measurements in iliac crest bone biopsies in 192 autopsy cases show that there is an only age-related bone loss but also a decrease in trabecular bonding. Through TBPf, we can show a significant difference in the age-related loss of trabecular connectivity between men and women.

Conventional electronic microscopes have acceleration potentials of several thousand volts and produce an electron beam penetrating into tissues and cellular cells (sections) of about 0.2 nm thick.

The development in the 1970s of high-voltage electronic microscopes capable of accelerating electrons over a potential of one million volts made it possible to study whole cell samples. Such microscopes are quite spectacular, usually occupying two floors of a laboratory (they are about 30 meters tall) and weigh about 20 tons.

Because the electron beam crosses the thickness of an entire cell, the inside of the cell is discovered in depth.

Mainly, due to the studies conducted by Porter, Schliwa, and Wolosewick Tucker, a high voltage microscope, it was demonstrated that the cytoplasm or matrix of eukaryotic

INDEPENDENT JOURNAL OF MANAGEMENT & PRODUCTION (IJM&P)
http://www.ijmp.jor.br *v. 11, n. 4, July - August 2020*
ISSN: 2236-269X
DOI: 10.14807/ijmp.v11i4.989

material is divided into two main phases: the micro-trabecular, intertrabecular network and spaces. A portion of the grid is observed in the high-voltage microphotography of Figure 1 and is schematically represented in Figure 2.

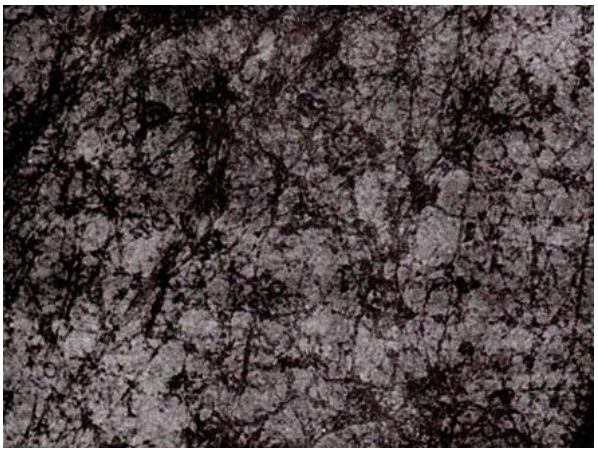

Figure 1: A portion of the grid is observed in the high-voltage microphotography.
Source: http://cdn.biologydiscussion.com/wp-content/uploads/2014/09/clip_image002140.jpg

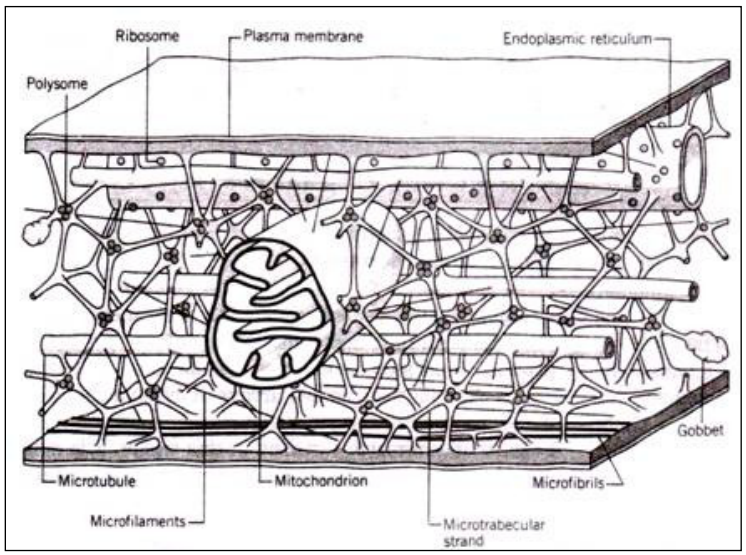

Figure 2: A model of the microtrabecular lattice.
Source: http://cdn.biologydiscussion.com/wp-content/uploads/2014/09/clip_image004108.jpg

The micro-trabecular grid is not a rigid or static structure. Rather, it varies in response to changes in cell activity and form. Its availability in a cell also varies in the cellular environment. For example, when cells are grown at a low temperature (eg 4 ° C), they become round to become spherical.

Changing the shape of the cell is due to a change in the cytoskeleton. First, disassemble the microtubules; then the cytoplasmic filaments disappear; and, finally, the microtrabecular are altered, although they do not decompose entirely.

ISSN: 2236-269X
DOI: 10.14807/ijmp.v11i4.989

The most important is the separation of some of the microtrabecular networks and their aggregation into gobbets (Figure 2). Loss of parts of the grid creates gaps that allow cellular organs to move more freely and also exhibit Brownian motion. If the cells are brought back to their normal (upper) temperature, the microtrabecular network, the cytoskeleton reform, and the organs are retained again in their movement.

Changes in the chemical composition of the environment in a cell also produce reversible changes in the network. Citochalazine B, a drug obtained from the helminthosporium dematoiderum matrix, determines microtrabecular narrowing. High or low osmotic pressure, changes in ion concentrations (eg Mg2 + and Ca2 +), as well as the presence of certain metabolic inhibitors also cause reversible changes in the network.

From a chemical point of view, the most important constituents of the network are proteins. Two-dimensional electrophoresis of lattice extracts suggests that more than 100 different proteins comprise this polymeric network.

The specific proteins that are supposed to be present are actin, myosin, and tubulin.

These proteins are also the main constituents of cytoplasmic filaments and microtubules.

A basic difference in the composition of microtrabecular and cytoskeletal elements (i.e. microtubules and cytoplasmic filaments) is disclosed when both are treated with organic detergents such as Triton X-100.

Triton X-100-treated cells lose microtrabecular wheat together with membrane structures, such as mitochondria, endoplasmic reticulum, plasma membrane, and nuclear envelope, but retain their cytoskeleton.

This behavior suggests that a microtrabecular has certain physical properties (and therefore a chemical composition) that are similar to those of membranes but unlike those of cytoskeletal elements.

Apparent microtubule galleries serve as an intracellular scaffold that helps suspend and organize the various structural components of the cytoplasm, including many cellular organs.

By acting in concert with cytoplasmic filaments and microtubules, the network plays an important role in maintaining cell shape and cellular movements.

There is also evidence suggesting that a range of intermediate metabolic enzymes, including glycolysis, is related to wheat.

ISSN: 2236-269X
DOI: 10.14807/ijmp.v11i4.989

These enzymes can be associated with the network in an orderly fashion; for example, the enzymes of a particular metabolic pathway may be linked to the network in such a way that the successive path reactions are spatially coordinated.

Today, the orthopedic prostheses used are mainly made of metals and ceramics with remarkable strength and stiffness, but with high physiological invasiveness. These systems, while guaranteeing biomechanical functionality, often interfere strongly with human bone physiology.

This invasiveness is particularly evident when replacement of hip joints using rigid metal prostheses.

Bicycle movement and vertical position should lead to unique and significant changes in the bone systems of the femur, pelvis, hip and lumbar vertebrae.

The complex evolution of trabecular bone positioning and morphology in the human proximal femur was mainly determined by stress patterns in which the bone was retained only in areas where it suffered sufficient mechanical stimuli and was lost when it was not (LOVEJOY, 1988; LOVEJOY, 2005; LOVEJOY et al., 2002).

Therefore, the clinical efficacy and long-term reliability of hip joint prostheses require a deeper understanding of the biomechanical invasiveness of current restoration replacements.

These products, which are made from traditional technologies such as melting and the mechanical machining, do not have flexible design solutions that allow optimal integration of the biomechanical bone into the complex bone of the femur. Moreover, these traditional solutions are not suitable for younger patients who have high life expectancy and then high prosthesis requirements in terms of biomechanical duration and osteointegration.

A new generation of prostheses with a better biomechanical bone osteointegration is needed.

In particular, additional technologies using titanium alloys or cobalt chromium due to their electricity in the process of generating high trabecular complex structures may represent the next generation of flexible production of trabecular biochemical prostheses.

Studies on prosthetic biomimetics involving these innovative manufacturing processes (ANNUNZIATA et al., 2006; APICELLA et al., 2010; AVERSA et al., 2009; AVERSA et al., 2016) have opened the definition of new design criteria for biomechanics compatible with prosthesis production (ANNUNZIATA et al., 2006; ANNUNZIATA et al., 2008; APICELLA

ISSN: 2236-269X
DOI: 10.14807/ijmp.v11i4.989

et al., 2010; APICELLA et al., 2011; APICELLA et al., 2015; GRAMANZINI et al., 2016; KUMMER, 1986; PERILLO et al., 2010; SORRENTINO et al., 2009, 2007; OH; HARRIS, 1976; GOTTESMAN; HASHIN, 1980; ASHMAN et al., 1984; DALSTYRA et al., 1993; ASHMAN; RHO, 1988, BURNSTEIN et al., 1976, CARTER; HAYES, 1977; AVERSA et al., 2009; AVERSA et al., 2016a; AVERSA et al., 2016b; AVERSA et al., 2016c; AVERSA et al., 2016d; AVERSA et al., 2016e; AVERSA et al., 2016f; AVERSA et al., 2016g; AVERSA et al., 2016h; AVERSA et al., 2016i; AVERSA et al., 2016j; AVERSA et al., 2016k; AVERSA et al., 2016l; AVERSA et al., 2016m; AVERSA et al., 2016n; AVERSA et al., 2016o; AVERSA et al., 2017; AVERSA et al., 2019; AVERSA AND APICELLA, 2014; BEAUPRE AND HAYES, 1985; BONFIELD et al., 1981; COMERUN, 1986; ČEPELAK, 2013; CHEN, 2013; CORMACK, 2012; DAVIS et al., 1991; DECHOW, 2003; FILMON et al., 2002; FROST, 1964; FROST, 1990; FROST, 2004; GORUSTOVICH et al., 2010; HALPIN; KARDOS, 1976; HEINEMANN et al., 2013; HUTMACHER, 2000; HOPPE et al., 2011; HENCH; WILSON, 1993; HENCH; POLAK, 2002; HENCH; THOMPSON, 2010; HUISKES et al., 1987; JULIEN et al., 2007; JONES; CLARE, 2012; KIM et al., 2004; KARAGEORGIOU; KAPLAN, 2005; KABRA et al., 1991; MANO et al., 2004; MIRSAYAR et al., 2017; MORALES-HERNANDEZ et al., 2012; MOURIÑO et al., 2012; MONTHEARD et al., 1992; PETRESCU, 2018; PETRESCU; CALAUTIT, 2016a; PETRESCU; CALAUTIT, 2016b; PETRESCU et al., 2015; PETRESCU et al., 2016a; PETRESCU et al., 2016b; PETRESCU et al., 2016c; PETRESCU et al., 2016d; PETRESCU et al., 2016e; PETRESCU et al., 2017; PETRESCU et al., 2018; PERILLO et al., 2010; PELUSO et al., 1997; PRASHANTHA et al., 2001; REILLY; BURNSTAIN, 1974; REILLY; BURNSTAIN, 1975; SCHIRALDI et al., 2004; SCHWARTZ-DABNEY; DECHOW, 2003; SORRENTINO et al., 2007; SORRENTINO et al., 2009; TÖYRÄSA et al., 2001; WOLFF, 1892; LOVEJOY, 1988; LOVEJOY, 2005; LOVEJOY et al., 2002; OJOVAN; LEE, 2010; KLEMENT et al., 1960; LIBERMANN; GRAHAM, 1976; ROYA; MAJUMDARA, 1981; INOUE et al., 2000; INOUE et al., 2011; REN et al., 2018; WANG et al., 2004; JOHNSON, 2002; LEWANDOWSKI et al., 2005; CHRISTOPHER et al., 2007).

2. METHODS AND MATERIALS

Figure 3 illustrates the biomimetic approach using silica, in vitro and in vivo validation steps for bone biofilm modelling.

INDEPENDENT JOURNAL OF MANAGEMENT & PRODUCTION (IJM&P)
http://www.ijmp.jor.br *v. 11, n. 4, July - August 2020*
ISSN: 2236-269X
DOI: 10.14807/ijmp.v11i4.989

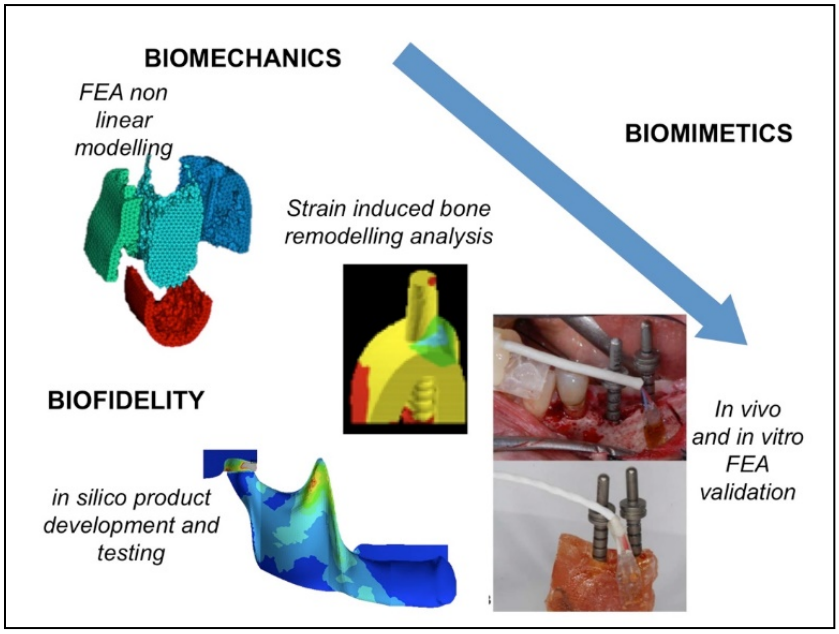

Figure 3: Biomimetic approach from bone biomechanics (mandible case study within silica, in vitro and in vivo validation steps)

The biophysical models of the mandible and the femur have been presented in previous publications (APICELLA et al., 2010; GRAMANZINI et al., 2016; PERILLO et al., 2010; SORRENTINO et al., 2007).

The authors of these studies investigated the untapped potential of additive manufacturing technologies. In addition, the progress of biomimetic design processes, which allowed us to conceptually develop a new biomimetic dental implant (AVERSA et al., 2009; AVERSA et al., 2016) and new trabecular prostheses could lead to new prosthetic systems imitating the biomechanical behavior of the femur (AVERSA et al., 2016).

The human femur has a small internal trabecular structure that optimizes the progressive and morphological mass types of trabecular bone and trabecula (WALKER et al., 1985; BRUNO et al., 1999; OH; HARRIS, 1978; TAMAR; HASHIN, 1980; TAMAR; HASHIN, 1984; DALSTRA et al., 1993).

Human bipedal swelling and vertical position have led to the unique and considerable adaptation of the axial systems of the femur, pelvis, hip and lumbar vertebrae. In particular, the hip joint gained a much wider position. The human femur, which is mainly loaded upright, evolved much more easily and more than for other primates where it is loaded horizontally.

This morphological evolution is due to the fact that the femoral neck of the limbs in the vertical support is loaded as a console and can then be linked to the less folded moments generated by humans.

INDEPENDENT JOURNAL OF MANAGEMENT & PRODUCTION (IJM&P)
http://www.ijmp.jor.br *v. 11, n. 4, July - August 2020*
ISSN: 2236-269X
DOI: 10.14807/ijmp.v11i4.989

The evolutionary pathway of the human hip was extensively reviewed (Lovejoi, 2005) to explain less the structure of the femoral prosthetic trabecular cortex, having cortical density densities determined only in specific locations (Figure 4 right).

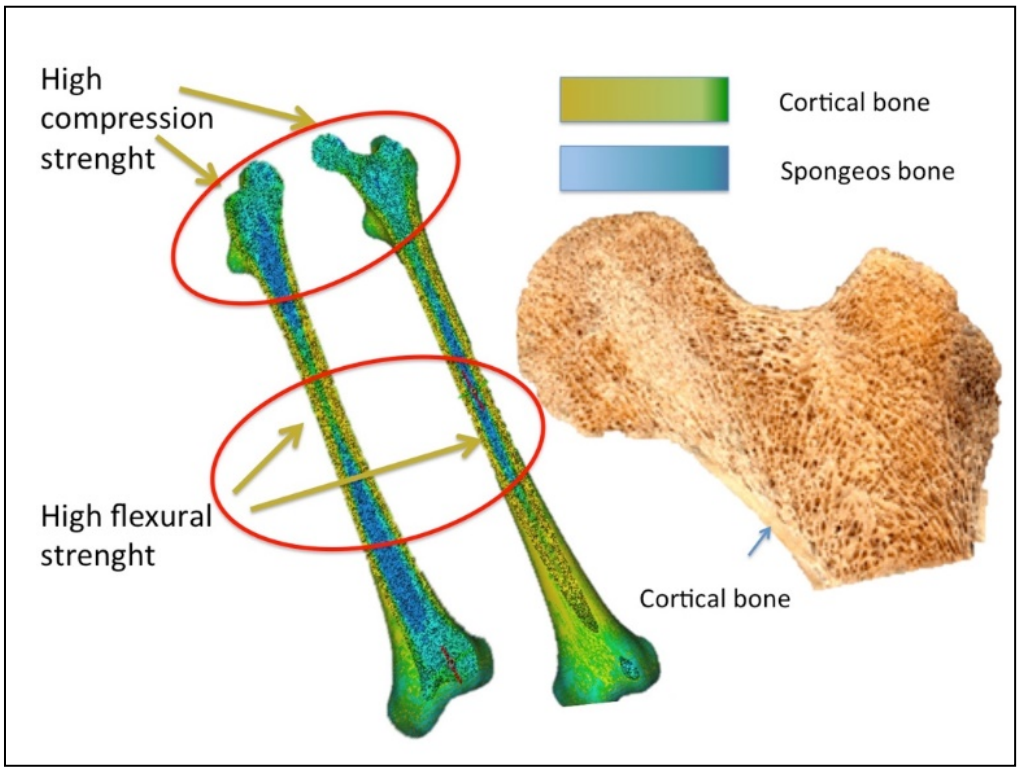

Figure 4: Cortical and trabecular bone distribution in the entire femur (left) and internal complex patterns of the trabecular bone in the proximal epiphysis section (right)

In particular, as shown in Ledyoy et al. (1988), the head of the femur thickened the cortex just below its lower portion, presenting at the same time an absence of the complete cortex at the tip of the femur, as shown in Figure 4 above.

In contrast, the very high cortical bone opposes the median diaphysis in which the stress of flexion predominates (Figure 4). Determining the complexity of the proximal position of the human femur in the trabecular bone morphology in the proximal femur (Figures 4 and 5), first of all, only bone rearrangement is retained in regions where there are sufficient stimuli to obtain a loss when not stretched and vice versa.

INDEPENDENT JOURNAL OF MANAGEMENT & PRODUCTION (IJM&P)
http://www.ijmp.jor.br *v. 11, n. 4, July - August 2020*
ISSN: 2236-269X
DOI: 10.14807/ijmp.v11i4.989

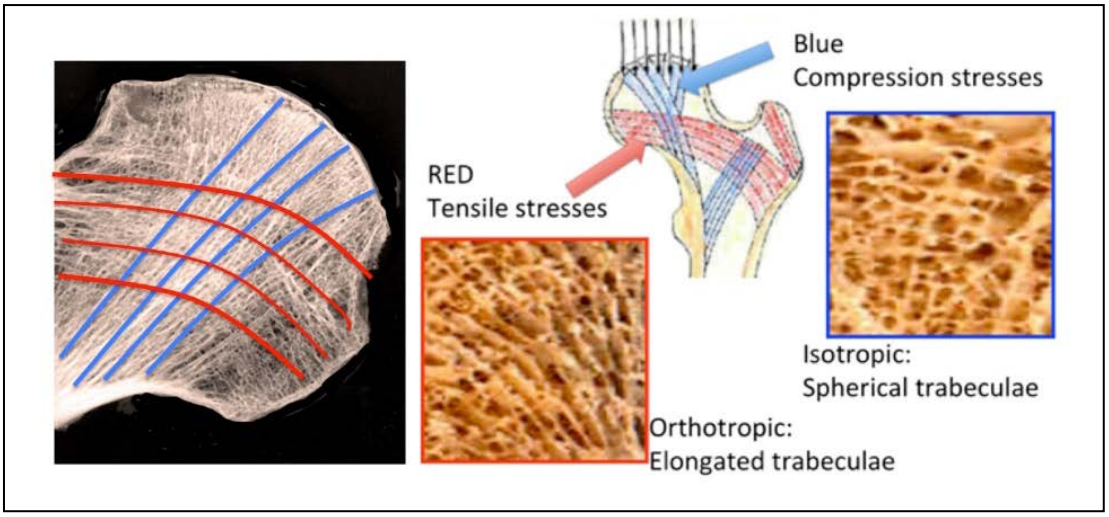

Figure 5: Radiographic evidence of oriented trabecular structure in compression (blue lines) and tensioned (red lines) and trabeculae isotropic (compression) and orthotropic (tension) morphology

Abscess attackers reduce the growth of upper thighs to such an extent that trabeculae coagulate by the progressive loss of arched trabeculae forming the Ward triangle, which is less radiopacity than that of other primates.

The trabecular bone morphology in the proximal epiphysis (the head of the femur) depends on the state of stress.

Figure 5 (left) shows the radiographic image of the epiphysis in which the trabecular orientation patterns for compressed lines (lines of blue) and traction lines (red lines) are clearly visible. Trabecular morphology in these two regions is completely different (Figure 5, right side): Spherical compression portions are observed because they are elongated intense regions. The mechanical behavior of these two structures is completely different: isotropic for spherical trabeculae and orthotropic (directional) for elongated trabeculae.

Solid models of trabecular structures obtained by micro transmitter tomography (Micro CT) in compressed regions (Figure 6a) and clogged (Figure 6c) clarify the origin of this different mechanical behavior. The repeat structure in the trabecular bone of the compressed regions consists of repeating the tetrahedral/octahedral units (Figure 6b). The more complex structure of the tensioned trabeculae (Figure 6c) is characterized by a different orientation and distribution in the cross sections (Figure 6d) and longitudinal (Figure 6e). This distribution, which is more continuous and massive in the longitudinal section, leads to greater resistance to bones and stiffness in the direction of trabecular orientation (Figure 6e) than in the transverse direction (Figure 6d).

INDEPENDENT JOURNAL OF MANAGEMENT & PRODUCTION (IJM&P)
http://www.ijmp.jor.br *v. 11, n. 4, July - August 2020*
ISSN: 2236-269X
DOI: 10.14807/ijmp.v11i4.989

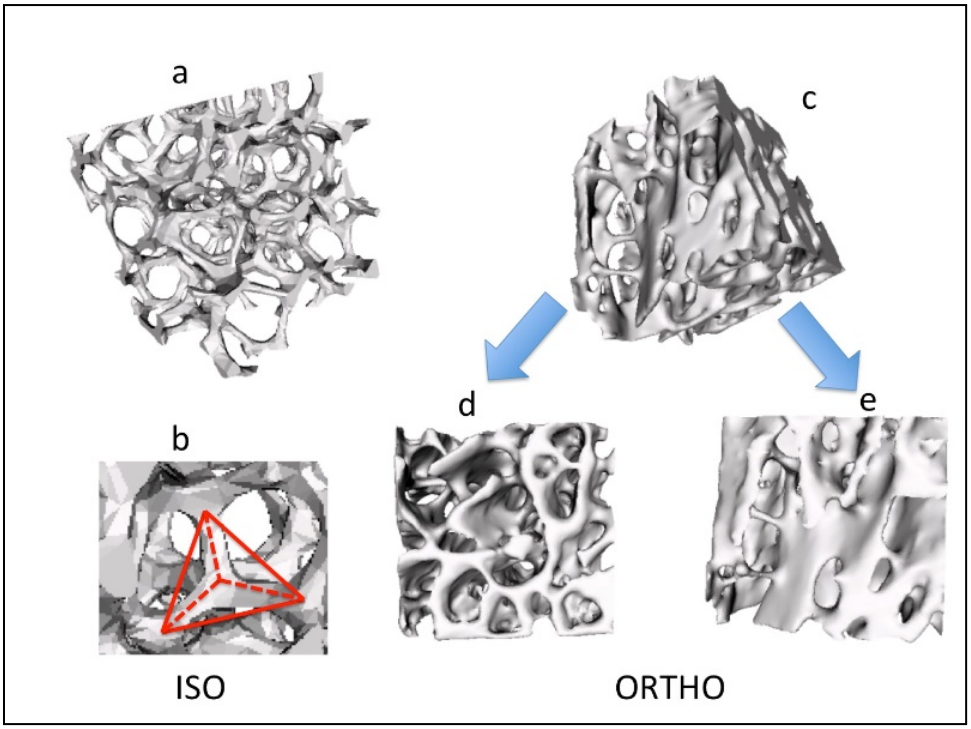

Figure 6: Solid models of femur iso (left) and ortho (right) bone trabecular structures from Micro CT of the femur

Full replacement of the hip in younger patients (under the age of 65) should be consistent with longer life expectancy, requiring prolonged prosthesis over 15 years. It is necessary to develop a biological and biomimetic prosthesis that combines the required force with the modulated stiffness that fits with that of the bone. The prosthesis replacing the cuts of the femoral head must provide an "equivalent stiffness" that can be achieved by combining the morphology and trabecular prosthesis that matches that of the missing part and by inducing an equivalent deformation of the residual bone region. Greater mechanical compatibility that allows for better bio- and osteointegration will increase life span, avoiding implant weakening and any additional surgical revision.

Figure 7 shows the adaptive bone properties that are in the coupling between bone formation and bone reabsorption.

This process refers to bone formation in which the osteoclast reabsorption through osteoclasts and the renewed generations of precursor osteoblasts replace the dynamic balance of the bone. The coupling can then be considered a complex mechanism of dynamic remodeling involving interactions of different types of cells and control stimuli.

INDEPENDENT JOURNAL OF MANAGEMENT & PRODUCTION (IJM&P)
http://www.ijmp.jor.br *v. 11, n. 4, July - August 2020*
ISSN: 2236-269X
DOI: 10.14807/ijmp.v11i4.989

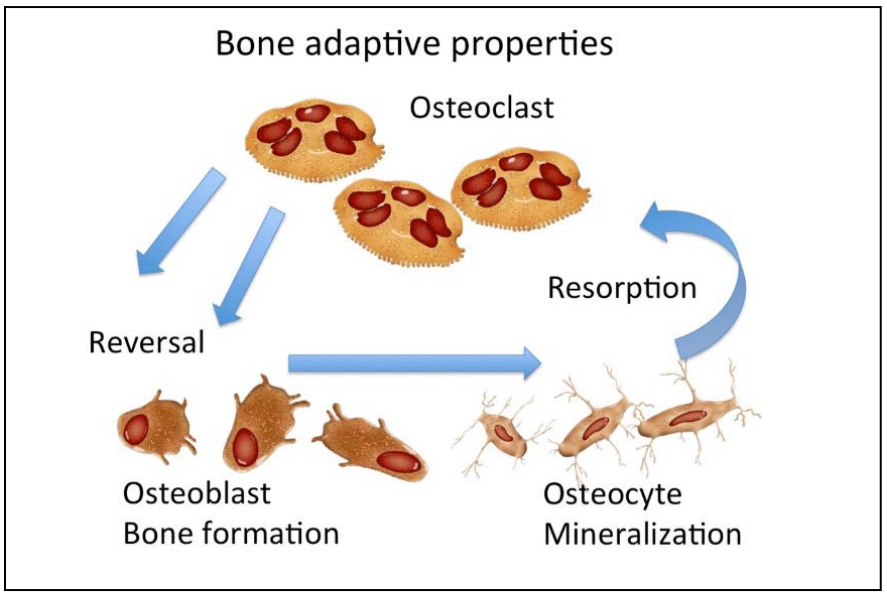

Figure 7: Bone adaptive properties: coupling between bone formation and bone reabsorption

Since bone remodeling takes place in several locations of the asynchronous skeleton, the mechanical control mechanisms are locally active (Figure 8). Mechanical stimulation should be between the physiological levels of the strain (Figure 8) between 50 μm and 3000 μm (APICELLA et al., 2011; APICELLA et al., 2015; AVERSA et al., 2009; AVERSA et al., 2016).

Osteoblasts under specific biochemical and mechanical stimuli mature and turn into osteocytes that mineralize the bone. The activity of osteoclasts under conditions that were not mechanically stimulated after the prosthesis could induce bone reabsorption in this new state of mechanical equilibrium.

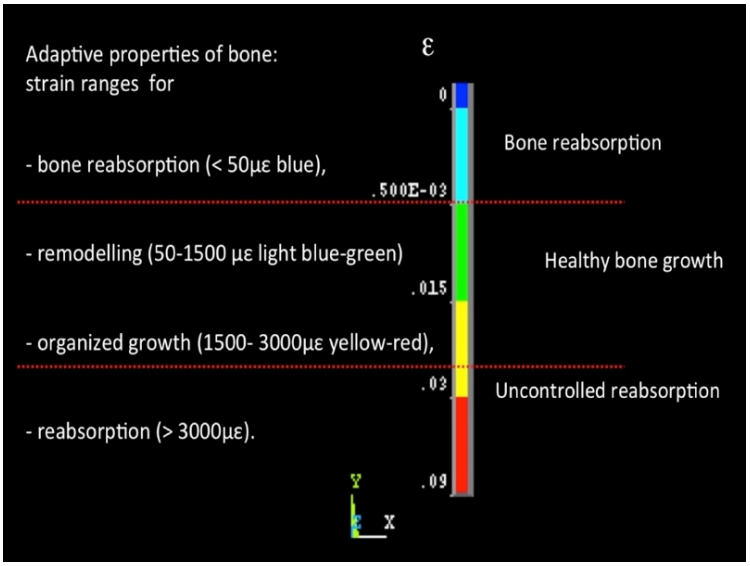

Figure 8: Bone adaptive properties: range of physiological strains for bone growth

ISSN: 2236-269X
DOI: 10.14807/ijmp.v11i4.989

The traditional full metal implants, adopted today, characterized by a much higher rigidity than the bone in which they are implanted, strongly alter the local physiological deformation leading to unwanted bone resorption. The incoherence of stiffness results in a low load, known as stress shielding, which reduces the physiological tension required for healthy bone growth (FROST, 1994, WEINANS et al., 1992). On the contrary, a personalized metal trabecular structure, combining the requirements of strength and elasticity, can produce a physiological mechanical stimulation of healthy growth, even in the prosthetic bone.

The trabecular metal structure of new prostheses could be made using electron sintered titanium alloys (EB). EB Additive technology melts titanium powders of about 50 microns that form thin layers over each other.

Furthermore, hybrid prostheses manufactured using hybrid polymeric materials (SCHIRALDI et al., 2004) can further improve bone biosynthesis and prostheses.

The new hybrid bioprosthesis could drastically reduce stress protection while providing an advantageous improvement in the life of the prosthesis compared to traditional solutions. Recovering optimal joint functionality will improve the quality of life of the patient, which perceives a significant reduction in the risk of new surgery.

In this study, the potential of new additive technologies in the development of trabecular prostheses, which mimics better the mechanical behavior of the resected bone, could lead to a new generation of biomimetic prostheses.

Finite element models were presented in previous papers in which the morphology of the structures of the femur and the mandible was evaluated (AVERSA et al., 2016; AVERSA et al., 2009; APICELLA et al., 2010; BEAUPRE; HAYES, 1985; REILLY; BURSTEIN, 1974; REILLY; BURSTEIN, 1975).

3. RESULTS AND DISCUSSION

Medical imaging segmentation was performed using the Mimics and 3Matic software (Materialize, Belgium) to process the CT and micro CT imaging of an entire femur and its proximal epiphysis, leading to the solid models reported in Figures 4 and 6 and STL, but in Figure 9.

ISSN: 2236-269X
DOI: 10.14807/ijmp.v11i4.989

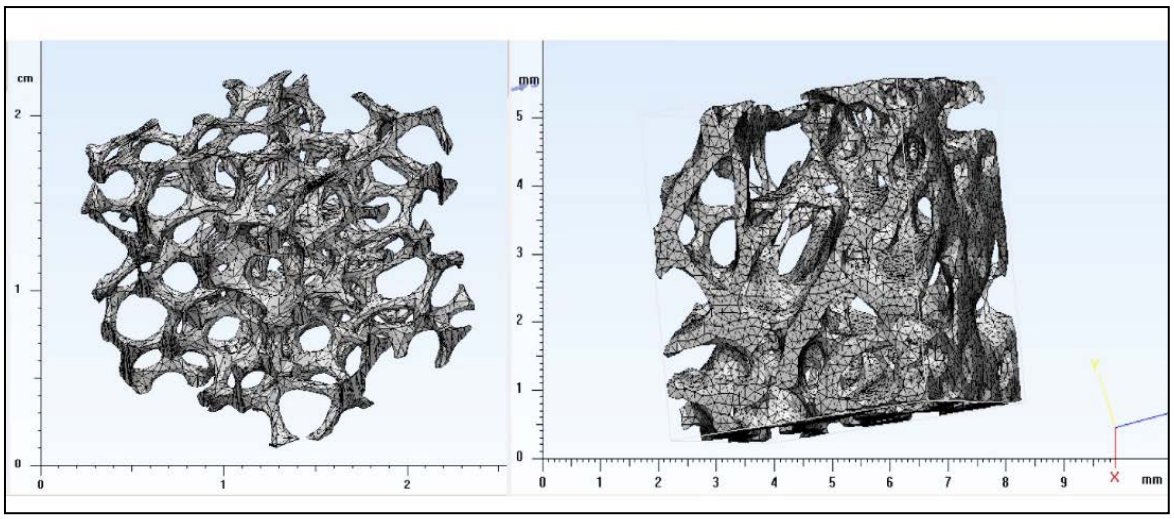

Figure 9: Discretized solid models for STL and FEA files generation

The results of the distribution of elemental tetrahedron material are shown in Figure 4. The green elements correspond to the cortical bone, while the light and dark blouses are relative to the trabecular bone. The same procedure was applied from Micro CT segmentation of the proximal sectional epiphysis (Figure 6) to the preparation of solid trabecular bone models, which characterize the micromorphology of the trabecular bone types of the femoral head.

The modeling of trabecular bone structures from Micro TAC segmentation was performed on a section of the dry femur (Figures 4 and 5). The trabecular bones of the femoral head, in fact, are characterized by different morphologies that are influenced by their position. In particular, a structure characterized by elongated asymmetrical pores in the direction of the stretching lines is evident in the areas subject to tension, while in the compressed areas the trabeculae follow a symmetrical arched structure.

The objective of modeling these regions was to identify the morphology and the exact properties of the trabecular structures to mimic the successive replication of the equivalent structures obtained through additive technology (see Figures 9 and 10), and Orthotropic orthotics (Figure 9, right side).

The solid CAD model and the massive massive mass asymmetric mass, which are expected to exhibit mechanical properties of an orthopedic structure, were obtained from MicroTac of a 4.5x4.5x4.5 mm trabecular segment processed with imitation material and 3Matic software.

Figure 9 (right side) shows a detailed surface (approximately 300,000 units) of trabecular structure (small size) of approximately 1,200 solid elements (4 knots of tetrahedral elements).

INDEPENDENT JOURNAL OF MANAGEMENT & PRODUCTION (IJM&P)
http://www.ijmp.jor.br *v. 11, n. 4, July - August 2020*
ISSN: 2236-269X
DOI: 10.14807/ijmp.v11i4.989

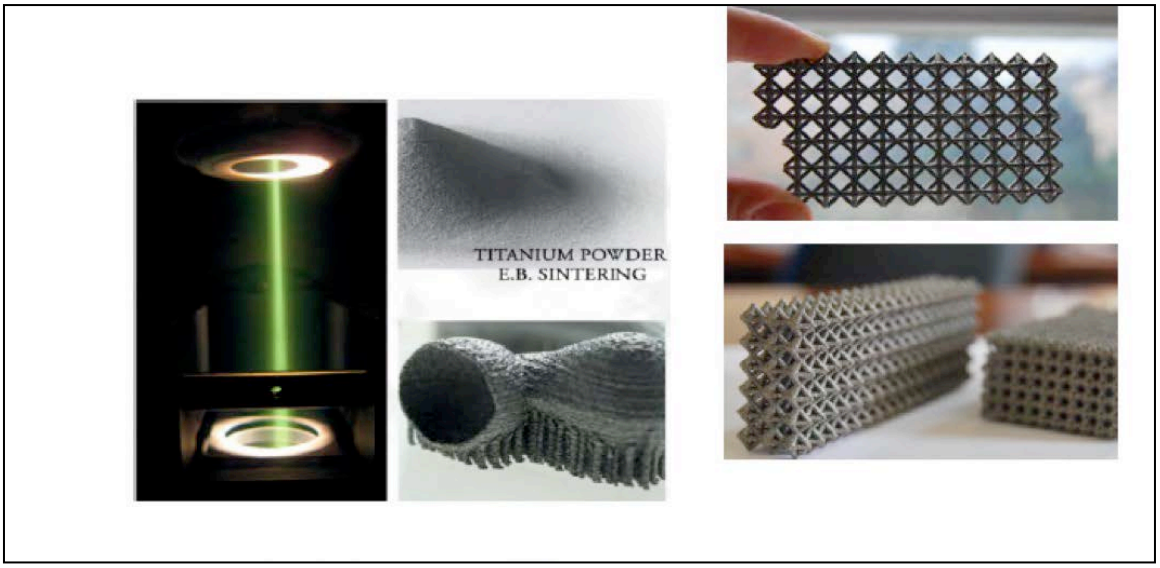

Figure 10: Biomimetic trabecular prostheses design from Ti powders sintering by Electron Beam Manufacturing

The apparent density of the trabecular bone, which was evaluated as a ratio of the occupied volume of the trachea (36.5 mm3) to the total occupied volume (103.7 mm3), is 0.665 grams per cm3 (this was assessed taking into account the cortical limit bone density of 1.9 g / cm3).

3.1. The isotropic trabecular part (Figure 9 on the left)

Similarly, the solid CAD model and symmetrical trabecular meshes expected to exhibit isotropic mechanical properties were obtained from the MicroTac segmentation of a 16x16x16 mm trabecular segment processed with Materialica Mimics and the 3Matic software. From this CAD surface model, the STL file and solid FEM model were generated by operating a 3matic volume network. The generated volume contains approximately 1900 tetrahedral elements and 31700 nodes. A bulk density of isotropic trabecular bone, derived from occupied trabecular volume (33167 mm3) at the total occupied volume (2340 mm3), with an apparent density of 0.070 g / cm3. Titan's equivalent isotropic and orthotropic structures will have apparent densities of 1.3 and 0.15 g / cm3. Equivalent structures to be used for the sintering of EB additives from Ti powder (Figure 10) is illustrated in Figure 11. Namely, an equation of tetrahedron equation for isotropic trabecular bone (Figure 11 left) and a tetrahedron with the three main 12 1 orthogonal (Figure 11 right) for the orthotropic tubular structure.

INDEPENDENT JOURNAL OF MANAGEMENT & PRODUCTION (IJM&P)
http://www.ijmp.jor.br *v. 11, n. 4, July - August 2020*
ISSN: 2236-269X
DOI: 10.14807/ijmp.v11i4.989

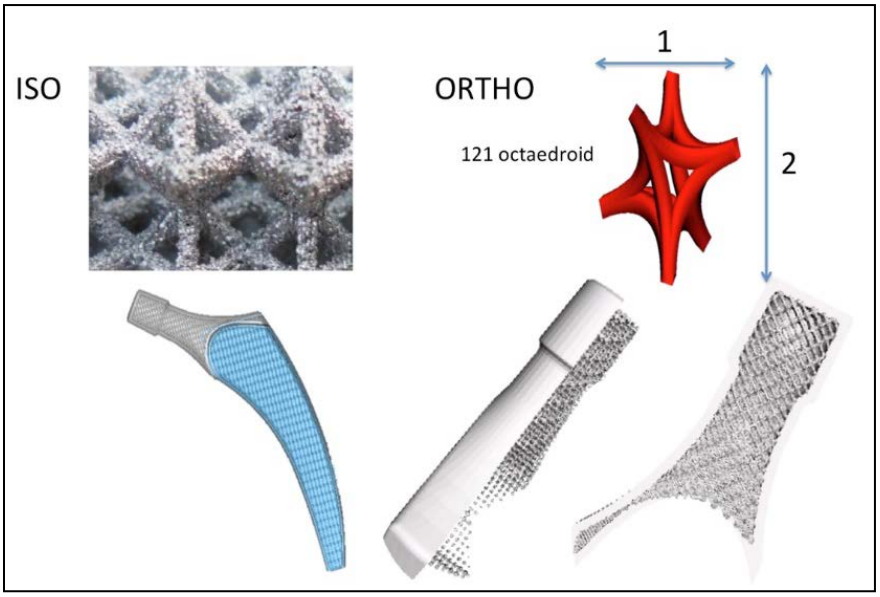

Figure 11: Trabecular prosthesis with iso (left, stem) and with ortho (right, head) structures.

3.2. Design with variable stiffness Ti

To reduce the stiffness of the prosthesis, a trabecular structure was designed to fit the rigidity specific to each diaphysis section interested in the prosthesis.

The proposed model of proximal hip epiphysis follows isostatic lines that characterize trabecular oriented systems (Kummer 1986) and is presented in Figure 11 (bottom).

The details of the trabecular prosthesis are shown in Figure 12.

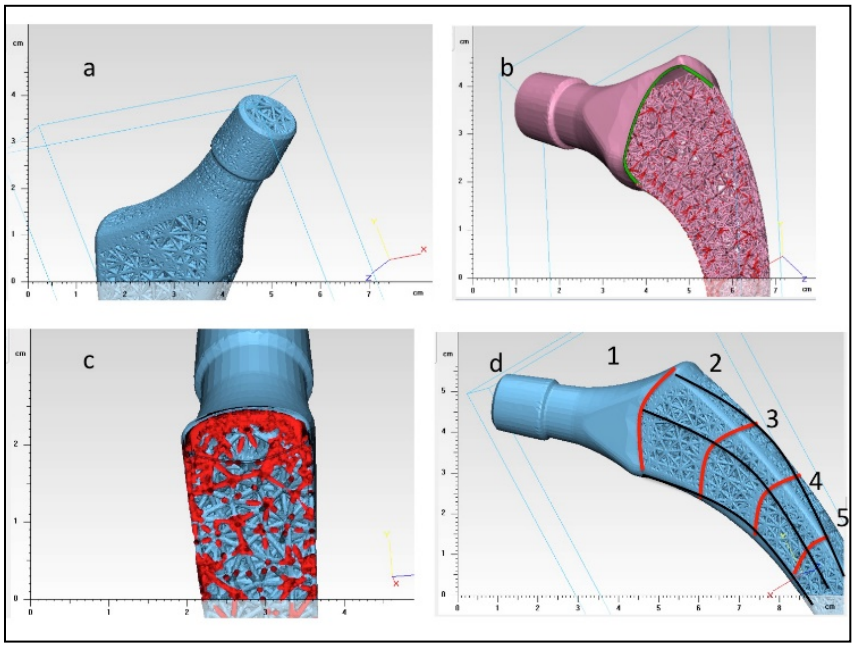

Figure 12: Flexible trabecular hip joint prosthesis with the trabecular structure obtained by additive sintering of Ti powders.
a) Internal trabecular structure of the prosthesis, b) Stem longitudinal section c) Stem transversal section, d) Isorigidity regions (red) and isotension lines (black)

ISSN: 2236-269X
DOI: 10.14807/ijmp.v11i4.989

The five regions of the decreasing stiffness of the prosthesis are contained in the red lines reported in the bottom right of Figure 12 along with the black lines.

These regions are characterized by different rigidities that progressively decrease from the highly rigid head (region 1 in Figure 12) down to the lower rigidity one (region 5 in Figure 11).

The orientation and shape of the trabecular porosity of the prosthesis are evident in the details of the internal structure reported in the transverse and longitudinal sections reported in Figure 12b and12c.

Isorigidity trabecular structure obtained by Ti alloy powder sintering by Electron Beam is reported in Figure 12d. The apparent elastic moduli of the trabecular structures are summarized in Table 1.

Table 1: Elastic modulus distribution in the isorigidity regions

Region	***1***	***2***	***3***	***4***	***5***
E, GPa	20.0	11.0	8.0	4.0	1.0

4. CONCLUSIONS

The proposed paper illustrates the new concept of biomimetic prostheses obtained using the trabecular structure in substitution of whole metal implants.

The currently used denture while the restoration of hip functionality does not maintain the physiological distribution of beneficial strains in the rest of the bone surrounding the prosthesis.

The most recent and most flexible biopsy can be completely biomimetic because they mimic and recapture the physiological distribution of the bone strain.

It could be expected that the new average duration of this flexible prosthesis would exceed the 10/15 years limits of the current prosthetic systems

This paper has identified design criteria and manufacturing technologies to exploit the potential of new personalized health care services. The new class of implants can be extended to orthopedics of the ankle, hip, and knee.

ISSN: 2236-269X
DOI: 10.14807/ijmp.v11i4.989

The new flexible prosthetic system allows for better functional recovery and bone regeneration due to their biomechanical activity.

Application of the product is possible surgical oncology for restoring the bone section of primitive and metastatic tumors.

5. ACKNOWLEDGEMENT

We thank Dr. Marco Sebastiani of the STM – Material Science and Technology Group at DIMI of Roma3 University ITALY and Dr. Paolo Bariani for technical support.

6. FUNDING INFORMATION

This research has been funded by Italian Ministry of University and Research project FIRB Future in Research 2008 project RBFR08T83J.

REFERENCES

ANNUNZIATA, M.; AVERSA, R.; APICELLA, A.; ANNUNZIATA, A.; APICELLA, D.; BUONAIUTO, C.; GUIDA, L. (2006) In vitro biological response to a light-cured composite when used for cementation of composite inlays, **Dental Materials**, v. 22, n. 12, p. 1081-1085. DOI: 10.1016/J.DENTAL.2005.08.009

ANNUNZIATA, M.; GUIDA, L.; PERILLO, L.; AVERSA, R.; I. PASSARO, I. (2008) Biological response of human bone marrow stromal cells to sandblasted titanium nitride-coated implant surfaces. **J. Mater. Sci. Mater. Med.**, v. 19, p. 3585-3591. DOI: 10.1007/s10856-008-3514-2.

APICELLA, D.; AVERSA, R.; FERRO, E.; IANNIELLO, D.; APICELLA, A. (2010) The importance of cortical bone orthotropicity, maximum stiffness direction and thickness on the reliability of mandible numerical models, **Journal of Biomedical Materials Research - Part B Applied Biomaterials**, v. 93, n. 1, p. 150-163 doi: 10.1002/jbm.b.31569

APICELLA, D.; VELTRI, M.; BALLERI, P.; APICELLA, A.; FERRARI, M. (2011) Influence of abutment material on the fracture strength and failure modes of abutment-fixture assemblies when loaded in a bio-faithful simulation, **Clinical Oral Implants Research**, v. 22, n. 2, p. 182-188: DOI: 10.1111/j.1600-0501.2010.01979.x

APICELLA, D.; AVERSA, R.; TATULLO, M.; SIMEONE, M.; SAYED, S.; MARRELLI, M.; APICELLA, A. (2015) Direct restoration modalities of fractured central maxillary incisors: A multi-levels validated finite elements analysis with in vivo strain measurements, **Dental Materials**, v. 31, n. 12, p. e289-e305, DOI: 10.1016/j.dental.2015.09.016

ASHMAN, R. B.; RHO, J. Y. (1988) Elastic modulus of trabecular bone material. **J. Biomechanics**, v. 21, p. 177-181. doi:10.1016/0021-9290(88)90167-4

ASHMAN, R. B.; COWIN, S. C.; VAN BUSKIRK, W. C.; RICE, J. C. (1984) A continuous wave technique for the measurement of the elastic properties of cortical bone, **J. Biomechanics**, v. 17, n. 5, p. 349-361, doi:10.1016/0021-9290(84)90029-0

AVERSA, R.; APICELLA, A. (2014) 3D analysis and nano-indentation mechanical characterization of a commercial Zr44-Ti11-Cu10-Ni10-Be25 metal glassy Alloy. **Advanced**

ISSN: 2236-269X
DOI: 10.14807/ijmp.v11i4.989

Materials Research.

AVERSA, R.; APICELLA, D.; PERILLO, L.; SORRENTINO, R.; ZARONE, F.; FERRARI, F.; APICELLA, A. (2009) Non-linear elastic three-dimensional finite element analysis on the effect of endocrown material rigidity on alveolar bone remodeling process. **Dental materials**, v. 25, p. 678–690. DOI: 10.1016/j.dental.2008.10.015

AVERSA, R.; PETRESCU, F. I. T.; PETRESCU, R. V.; APICELLA, A. (2016a) Biomimetic FEA bone modeling for customized hybrid biological prostheses development. **Am. J. Applied Sci.,** v. 13, p. 1060-1067. DOI: 10.3844/ajassp.2016.1060.1067

AVERSA, R.; PARCESEPE, D.; PETRESCU, R. V.; CHEN, G.; PETRESCU, F. I. T.; TAMBURRINO, F.; APICELLA, A. (2016b) Glassy Amorphous Metal Injection Molded Induced Morphological Defects, **Am. J. Applied Sci.**, v. 13, n. 12, p. 1476-1482.

AVERSA, R.; PETRESCU, R. V.; PETRESCU, F. I. T.; APICELLA, A. (2016c) Smart-Factory: Optimization and Process Control of Composite Centrifuged Pipes, **Am. J. Applied Sci.**, v. 13, n. 11, p. 1330-1341.

AVERSA, R.; TAMBURRINO, F.; PETRESCU, R. V.; PETRESCU, F. I. T.; ARTUR, M.; CHEN, G.; APICELLA, A. (2016d) Biomechanically Inspired Shape Memory Effect Machines Driven by Muscle like Acting NiTi Alloys, **Am. J. Applied Sci.**, v. 13, n. 11, p. 1264-1271.

AVERSA, R.; BUZEA, E. M.; PETRESCU, R. V.; APICELLA, A.; NEACSA, M.; PETRESCU, F. I. T. (2016e) Present a Mechatronic System Having Able to Determine the Concentration of Carotenoids, **Am. J. of Eng. and Applied Sci.**, v. 9, n. 4, p. 1106-1111.

AVERSA, R.; PETRESCU, R. V.; SORRENTINO, R.; PETRESCU, F. I. T.; APICELLA, A. (2016f) Hybrid Ceramo-Polymeric Nanocomposite for Biomimetic Scaffolds Design and Preparation, **Am. J. of Eng. and Applied Sci.**, v. 9, n. 4, p. 1096-1105.

AVERSA, R.; PERROTTA, V.; PETRESCU, R. V.; MISIANO, C.; PETRESCU, F. I. T.; APICELLA, A. (2016g) From Structural Colors to Super-Hydrophobicity and Achromatic Transparent Protective Coatings: Ion Plating Plasma Assisted TiO2 and SiO2 Nano-Film Deposition, **Am. J. of Eng. and Applied Sci.**, v. 9, n. 4, p. 1037-1045.

AVERSA, R.; PETRESCU, R. V.; PETRESCU, F. I. T.; APICELLA, A. (2016h) Biomimetic and Evolutionary Design Driven Innovation in Sustainable Products Development, **Am. J. of Eng. and Applied Sci.**, v. 9, n. 4, p. 1027-1036.

AVERSA, R.; PETRESCU, R. V.; APICELLA, A.; PETRESCU, F. I. T. (2016i) Mitochondria are Naturally Micro Robots - A review, **Am. J. of Eng. and Applied Sci.**, v. 9, n. 4, p. 991-1002.

AVERSA, R.; PETRESCU, R. V.; APICELLA, A.; PETRESCU, F. I. T. (2016j) We are Addicted to Vitamins C and E-A Review, **Am. J. of Eng. and Applied Sci.**, v. 9, n. 4, p. 1003-1018.

AVERSA, R.; PETRESCU, R. V.; APICELLA, A.; PETRESCU, F. I. T. (2016k) Physiologic Human Fluids and Swelling Behavior of Hydrophilic Biocompatible Hybrid Ceramo-Polymeric Materials, **Am. J. of Eng. and Applied Sci.**, v. 9, n. 4, p. 962-972.

AVERSA, R.; PETRESCU, R. V.; APICELLA, A.; PETRESCU, F. I. T. (2016l) One Can Slow Down the Aging through Antioxidants, **Am. J. of Eng. and Applied Sci.**, v. 9, n. 4, p. 1112-1126.

ISSN: 2236-269X
DOI: 10.14807/ijmp.v11i4.989

AVERSA, R.; PETRESCU, R. V.; APICELLA, A.; PETRESCU, F. I. T. (2016m) About Homeopathy or ≪Similia Similibus Curentur≫, **Am. J. of Eng. and Applied Sci.**, v. 9, n. 4, p. 1164-1172.

AVERSA, R.; PETRESCU, R. V.; APICELLA, A.; PETRESCU, F. I. T. (2016n) The Basic Elements of Life's, **Am. J. of Eng. and Applied Sci.**, v. 9, n. 4, p. 1189-1197.

AVERSA, R.; PETRESCU, F. I. T.; PETRESCU, R. V.; APICELLA, A. (2016o) Flexible Stem Trabecular Prostheses, **Am. J. of Eng. and Applied Sci.**, v. 9, n. 4, p. 1213-1221.

AVERSA, R.; PETRESCU, R. V. V.; APICELLA, A.; PETRESCU, F. I. T. (2017) Modern Transportation and Photovoltaic Energy for Urban Ecotourism. **Transylvanian Review of Administrative Sciences**, Special n.; p. 5-20. DOI: 10.24193/tras.SI2017.1

AVERSA, R.; PETRESCU, R. V. V.; APICELLA, A.; PETRESCU, F. I. T. (2019) A Nanodiamond for Structural Biomimetic Scaffolds. **Engineering Review**, v. 39, n. 1, p. 81-89. DOI: http://doi.org/10.30765/er.39.1.9

BEAUPRE, G. S.; HAYES, W. C. (1985) Finite Element Analysis of a three dimensional open-celled model for trabecular bone. **J. Biomech. Eng.**, v. 107, p. 249-56, PMID: 4046566

BONFIELD, W.; GRYNPAS, M. D.; TULLY, A. E.; BOWMAN, J.; ABRAM, J. (1981) Hydroxyapatite reinforced polyethylene — a mechanically compatible implant material for bone replacement. **Biomaterials**, v. 2, p. 185-186. DOI: 10.1016/0142-9612(81)90050-8

BRUNO, R. J.; SAUER, P. A.; ROSENBERG, A. G.; BLOCK, J.; SUMNER, D. R. (1999) The pattern of bone mineral density in the proximal femur and radiographic signs of early joint degeneration. **J Rheumatol**, v. 26, p. 636–640

BURNSTEIN, A.; REILLY, D. T.; MARTENS, M. (1976). Aging of bone tissue: Mechanical properties.; **J. of Bone and joint Surgery**, v. 58, p. 82-86, https://www.researchgate.net/publication/21906817_Aging_of_Bone_Tissue_Mechanical_Properties

CARTER, D. R.; HAYES, W. C. (1977) The compressive behavior of bone as a two phase porous structure. **J. of Bone and joint Surgery,** v. 59a, p. 954, PMID: 561786

ČEPELAK, I.; DODIG, S.; ČULIĆ, O. (2013) Magnesium-more than a common cation. **Med. Sci.**, v. 39, p. 47-68.

CHEN, Q.; ZHU, C.; THOUAS, G. A. (2012) Progress and challenges in biomaterials used for bone tissue engineering: Bioactive glasses and elastomeric composites. Progress. **Biomater.**, v. 1, n. 1-22. DOI: 10.1186/2194-0517-1-2

CHRISTOPHER, A.; SCHUH, T. C.; HUFNAGEL, U. R. (2007) Mechanical behavior of amorphous alloys, **Acta Materialia**, v. 55, n. 4067.

COMERUN, H. U. (1986) Six-year results with a microporous-coated metal hip prosthesis, **Clin. Orthop.**, v. 208, n. 81.

CORMACK, A. N.; TILOCCA, A. (2012) Structure and biological activity of glasses and ceramics. **Philos. Trans. Math. Phys. Eng. Sci.**, v. 370, p. 1271-1280. DOI: 10.1098/rsta.2011.0371

DALSTRA, M.; HUISKES, R.; ODGAARD, A.; VAN ERNING, L. (1993) Mechanical and textural properties of Pelvic Trabecular Bone. **J. Biomechanics**, v. 26, n. 4-5, p. 349-361, DOI: 10.1016/0021-9290(93)90014-6

DAVIS, P. A.; HUANG, S. J.; NICOLAIS, L.; AMBROSIO, L. (1991) Modified PHEMA

ISSN: 2236-269X
DOI: 10.14807/ijmp.v11i4.989

Hydrogels. In: Szycher M, editor. High performance biomaterials. Lancaster, PA, USA: **Technonic**. p. 343–68.

FILMON, R.; GRIZON, F.; BASLIE, M. F.; CHAPPARD, D. (2002) Effects of negatively charged groups (carboxymethyl) on the calcification of poly(2-hydroxyethylmethacrylate). **Biomaterials**, v. 23, p. 3053–9.

FROST, H. M. (1964) Mathematical elements of lamellar bone remodeling. **Springfield: Charles C Thomas**, p. 22–25.

FROST, H. M. (1990) Structural adaptations to mechanical usage (SATMU). 2. Redifining Wolff's law: the bone remodelling problem. **Anat Rec**, v. 226, p. 414–22.

FROST, H. M. (2003) update of bone physiology and Wolff's law for clinicians. **Angle Orthod**, v. 74, p. 3–15.

FROST, H. M. (1994) Wolff's law and bone's structural adaptations to mechanical usage: an overview for clinicians. **Angle Orthod**, v. 64, p. 175–88.

GRAMANZINI, M.; GARGIULO, S.; ZARONE, F.; MEGNA, R.; APICELLA, A.; AVERSA, R.; SALVATORE, M.; MANCINI, M.; SORRENTINO, R.; BRUNETTI, A. (2016) Combined microcomputed tomography, biomechanical and histomorphometric analysis of the peri-implant bone: A pilot study in minipig model. **Dental Materials**, v. 32, n. 6, p. 794-806: DOI: 10.1016/j.dental.2016.03.025

GORUSTOVICH, A. A.; ROETHER, J. A.; BOCCACCINI, A. R. (2010) Effect of bioactive glasses on angiogenesis: A review of *in vitro* and *in vivo* evidences. **Tissue Eng. Part B Rev.**, v. 16, p. 199-207. DOI: 10.1089/ten.TEB.2009.0416

HALPIN, J. C.; KARDOS, J. L. (1976) Halpin-Tsai equations: A review, **Polymer Engineering and Science**, v. 16, n. 5, p. 344-352

HEINEMANN, S.; HEINEMANN, C.; WENISCH, S.; ALT, V.; WORCH, H. (2013) Calcium phosphate phases integrated in silica/collagen nanocomposite xerogels enhance the bioactivity and ultimately manipulate the osteoblast/osteoclast ratio in a human co-culture model. **Acta Biomaterialia**, v. 9, p. 4878-4888. DOI: 10.1016/j.actbio.2012.10.010

HENCH, L. L.; POLAK, J. M. (2002) Third-generation biomedical materials. **Science**, v. 295, p. 1014-1017. DOI: 10.1126/science.1067404

HENCH, L. L.; THOMPSON, I. (2010) Twenty-first century challenges for biomaterials. **J. Royal Society Interface**, v. 7, p. S379-S391. DOI: 10.1098/rsif.2010.0151.focus

HENCH, L. L.; WILSON, J. (1993) An introduction to bioceramics. **World Sci.**, v. 1, p. 396-396. DOI: 10.1142/2028

HOPPE, A.; GÜLDAL, N. S.; BOCCACCINI, A. R. (2011) A review of the biological response to ionic dissolution products from bioactive glasses and glass-ceramics. **Biomaterials**, v. 32, p. 2757-2774. DOI: 10.1016/j.biomaterials.2011.01.004

HUISKES, R.; WEINANS, H.; GROOTENBOER, H. J.; DALSTRA, M.; FUDULA, B.; SLOOFF, T. J. (1987) Adaptive bone remodeling theory applied to prosthetic-design analysis. **J Biomech**, v. 20, p. 1135–1150.

HUTMACHER, D. W. (2000) Scaffolds in tissue engineering bone and cartilage. **Biomaterials,** v. 21, p. 2529-2543. DOI: 10.1016/S0142-9612(00)00121-6

ISSN: 2236-269X
DOI: 10.14807/ijmp.v11i4.989

INOUE, A.; SOBU, S.; LOUZGUINE, D. V.; KIMURA, H.; SASAMORI, K. (2011) "Ultrahigh strength Al-based amorphous alloys containing Sc". **Journal of Materials Research**, v. 19, n. 5, p. 1539. Doi:10.1557/JMR.2004.0206.

INOUE A. (2000) Stabilization of metallic supercooled liquid and bulk amorphous alloys, **Acta Mater**, v. 48, p. 279.

JONES, J. R.; CLARE, A. G. (2012) Bio-Glasses. An Introduction. 1st Edn.; **Wiley, Chichester,** ISBN-10: 1118346475, p. 320.

JOHNSON, W. L. (2002) Bulk amorphous metal – an emerging engineering material, **JOM**, v. 54, p. 40.

JULIEN, M.; MAGNE, D.; MASSON, M.; ROLLI-DERKINDEREN, M.; CHASSANDE, O. (2007) Phosphate stimulates matrix Gla protein expression in chondrocytes through the extracellular signal regulated kinase signaling pathway. **Endocrinology**, v. 148, p. 530-537. DOI: 10.1210/en.2006-0763

KABRA, B.; GEHRKE, S. H.; HWANG, S. T.; RITSCHEL, W. (1991) Modification of the dynamic swelling behaviour of pHEMA. **J Appl Polym Sci**, v. 42, p. 2409–16.

KARAGEORGIOU, V.; KAPLAN, D. (2005) Porosity of 3D biomaterial scaffolds and osteogenesis. **Biomaterials**, v. 26, p. 5474-5491. DOI: 10.1016/j.biomaterials.2005.02.002

KIM, H. W.; KNOWLES, J. C.; KIM, H. E. (2004) Development of hydroxyapatite bone scaffold for controlled drug release via poly(ϵ-caprolactone) and hydroxyapatite hybrid coatings. **J. Biomed. Mater. Res. Part B: Applied Biomater.**, v. 70, p. 240-249. DOI: 10.1002/jbm.b.30038

KLEMENT, W.; WILLENS, R. H.; DUWEZ, P. O. L. (1960) Non-crystalline Structure in Solidified Gold-Silicon Alloys. **Nature**, v. 187, n. 4740, p. 869–870. Doi:10.1038/187869b0.

KUMAR, A.; RATHI, A.; SINGH, J.; SHARMA, N. K. (2016) Studies on Titanium Hip Joint Implants using Finite Element Simulation. In **Proceedings of the World Congress on Engineering**, v. 2.

KUMMER, B. (1986) Biomechanical principles of the statistics of the hip joint. A critical appraisal of a new theory, **Zeitschrift fur Orthopadie und Ihre Grenzgebiete**, v. 124, n. 2, p. 179-187.

LEWANDOWSKI, J. J.; WANG, W. H.; GREER, A. L. (2005) Intrinsic plasticity or brittleness of metallic glasses, **Philos Mag Lett**, v. 85, p. 77.

LIBERMANN, H.; GRAHAM C. (1976) Production Of Amorphous Alloy Ribbons And Effects Of Apparatus Parameters On Ribbon Dimensions. **IEEE Transactions on Magnetics**, v. 12, n. 6, p. 921. Doi:10.1109/TMAG.1976.1059201.

LOVEJOY, C. O. (2005) The natural history of human gait and posture. Part 2. Hip and thigh, **Gait & Posture**, v. 21, n. 1, p. 113-24, DOI: 10.1016/j.gaitpost.2004.06.010

LOVEJOY, C. O. (1988) Evolution of human walking. **Sci Am**., n. 259, p. 118-125.

LOVEJOY, C. O.; MEINDL, R. S.; OHMAN, J. C.; HEIPLE, K. G.; WHITE, T. D. (2002) The Maka femur and its bearing on the antiquity of human walking: applying contemporary concepts of morphogenesis to the human fossil record. **Am J Phys Anthropol**, v. 119, p. 97–133.

MANO, J. F.; SOUSA, R. A.; BOESEL, L. F.; NEVES, N. M.; REIS, R. L. (2004) Bioinert, biodegradable and injectable polymeric matrix composites for hard tissue replacement: State

ISSN: 2236-269X
DOI: 10.14807/ijmp.v11i4.989

of the art and recent developments. **Composi. Sci. Technol.**, v. 64, p. 789-817. DOI: 10.1016/j.compscitech.2003.09.001

MAZAHERI, M.; HASSANI, K.; KARIMI, A.; IZADI, F. (2016) Finite Element Study of Composite Materials as an Alternative for Metal Hip Prothesis Using Variable Load. **Materials Focus**, v. 5, n. 5, p. 430-435.

MIRSAYAR, M. M.; PARK, P. (2016) Modified maximum tangential stress criterion for fracture behavior of zirconia/veneer interfaces. **Journal of the mechanical behavior of biomedical materials**, v. 59, p. 236-240.

MIRSAYAR, M. M.; JONEIDI, V. A.; PETRESCU, R. V. V.; PETRESCU, F. I. T.; BERTO, F. (2017) Extended MTSN criterion for fracture analysis of soda lime glass, **Engineering Fracture Mechanics** v. 178, p. 50–59, ISSN: 0013-7944, http://doi.org/10.1016/j.engfracmech.2017.04.018

MORALES-HERNANDEZ, D. G.; GENETOS, D. C.; WORKING, D. M.; MURPHY, K. C.; LEICH, J. K. (2012) Ceramic identity contributes to mechanical properties and osteoblast behavior on macroporous composite scaffolds. **J. Funct. Biomat.**, v. 23, p. 382-397. DOI: 10.3390/jfb3020382

MOURIÑO, V.; CATTALINI, J. P.; BOCCACCINI, A. R. (2012) Metallic ions as therapeutic agents in tissue engineering scaffolds: An overview of their biological applications and strategies for new developments. **J. Royal Society Interface**, v. 9, p. 401-419. DOI: 10.1098/rsif.2011.0611

MONTHEARD, J. P.; CHATZOPOULOS, M.; CHAPPARD, D. (1992) 2-hydroxyethylmethacrylate HEMA; chemical properties and applications in biomedical fields. **J Macromol Sci Macromol Rev**., v. 32, p. 1–34.

MULLENDER, M. G.; HUISKES, R. (1995) A proposal for the regulatory mechanism of Wolff's law. **J Orthop Res**., v. 13, p. 503–512. DOI: 10.1002/jor.1100130405

OH, I.; HARRIS, W. H.; (1976) Proximal distribution in the loaded femur. **J. of Bone and Joint Surgery**, v. 60-A, n. 1. PMID: 624762. https://www.researchgate.net/publication/21906817_Aging_of_Bone_Tissue_Mechanical_Properties

OJOVAN, M. I.; LEE, W. B. E. (2010) Connectivity and glass transition in disordered oxide systems. **Journal of Non-Crystalline Solids**., v. 356, n. 44–49, p. 2534. Doi:10.1016/j.jnoncrysol.2010.05.012.

PELUSO, G.; PETILLO, O.; ANDERSON, J. M.; AMBROSIO, M.; NICOLAIS, L.; MELONE, M. A. B.; ESCHBACH, F. O.; HUANG, S. J.; (1997) The differential effects of poly(2-hydroxyethylmethacrylate) and poly(2-hydroxyethylmethacrylate)/poly(caprolactone) polymers on cell proliferation and collagen synthesis by human lung fibroblasts. **J Biomed Mater Res**., v. 34, p. 327–36.

PERILLO, L;. SORRENTINO, R.; APICELLA, D.; QUARANTA, A.; GHERLONE, E. D.; FERRARI, M.; AVERSA, R.; APICELLA, A. (2010) Nonlinear visco-elastic finite element analysis of porcelain veneers: a submodelling approach to strain and stress distributions in adhesive and resin cement. **The journal of adhesive dentistry**, v. 12, n. 5, p. 403-413: ISSN: 14615185

PETRESCU, F. I. T.; CALAUTIT, K. J. (2016a) About Nano Fusion and Dynamic Fusion, **Am. J. Applied Sci.**, v. 13, n. 3, p. 261-266.

ISSN: 2236-269X
DOI: 10.14807/ijmp.v11i4.989

PETRESCU, F. I. T.; CALAUTIT, K. J. (2016b) About the Light Dimensions, **Am. J. Applied Sci**., v. 13, n. 3, p. 321-325.

PETRESCU, F. L.; BUZEA, E.; NĂNUŢ, L.; NEACŞA, M.; NAN, C. (2015) The role of antioxidants in slowing aging of skin in a human, **Analele Univers. Craiova Biologie Horticultura Tehn. Prel. Prod. Agr. Ing. Med.**, v. 20, p. 567-574.

PETRESCU, F. I. T.; APICELLA, A.; AVERSA, R.; PETRESCU, R. V.; CALAUTIT, J. K.; MIRSAYAR, M. (2016a) Something about the Mechanical Moment of Inertia, **Am. J. Applied Sci.**, v. 13, n. 11, p. 1085-1090.

PETRESCU, R. V.; AVERSA, R.; APICELLA, A.; LI, S.; CHEN, G.; MIRSAYAR, M.; PETRESCU, F. I. T. (2016b) Something about Electron Dimension, **Am. J. Applied Sci.**, v. 13, n. 1, p. 1272-1276.

PETRESCU, R. V.; AVERSA, R.; APICELLA, A.; BERTO, F.; LI, S.; PETRESCU, F. I. T. (2016c) Ecosphere Protection through Green Energy, **Am. J. Applied Sci.**, v. 13, n. 10, p. 1027-1032.

PETRESCU, F. I. T.; APICELLA, A.; PETRESCU, R. V.; KOZAITIS, S. P.; BUCINELL, R. B.; AVERSA, R.; ABU-LEBDEH, T. M. (2016d) Environmental Protection through Nuclear Energy, **Am. J. Applied Sci.**, v. 13, n. 9, p. 941-946.

PETRESCU, R. V.; AVERSA, R.; APICELLA, A.; PETRESCU, F. I. T. (2016e) Future Medicine Services Robotics, **Am. J. of Eng. and Applied Sci.**, v. 9, n. 4, p. 1062-1087.

PETRESCU, F. I. T.; PETRESCU, R. V.; MIRSAYAR, M. M. (2017) The Computer Algorithm for Machine Equations of Classical Distribution. **Journal of Materials and Engineering Structures**, v. 4, n. 4, p. 193-209. http://revue.ummto.dz/index.php/JMES/article/view/1590

PETRESCU, F. I. T.; PETRESCU, R. V.; MIRSAYAR, M. M. (2018) Inverse Kinematics to a Stewart Platform. **Journal of Materials and Engineering Structures**, v. 5, n. 2, p. 111-122. http://revue.ummto.dz/index.php/JMES/article/view/1623

PETRESCU, F. I. T. (2019) About the nuclear particles' structure and dimensions. **Comp. Part. Mech**., v. 6, p. 191-194, https://doi.org/10.1007/s40571-018-0206-7

PRASHANTHA, K.; VASANTH, K. P. K.; SHERIGARA, B. S.; PRASANNAKUMAR, S. (2001) Interpenetrating polymer networks based on polyol modified castor oil polyurethane and poly-(2-hydroxyethylmethacrylate): synthesis, chemical, mechanical and thermal properties, bull. **Mater Sci**., v. 24, n. 5, p. 535–8.

REILLY, D.; BURSTEIN, A. H. (1974) The mechanical properties of cortical bone. **The J. Of bone and Joint Surgery**, v. 56A, n. 5, p. 1001-1021

REILLY, D. T.; BURNESTAIN, A. H. (1975) The elastic and ultimate properties of compact bone tissue. **J. Biomechanics**, v. 8, p. 393-405, doi:10.1016/0021-9290(75)90075-5

REN, F.; WARD, L.; WILLIAMS, T.; LAWS, K. J.; WOLVERTON, C.; HATTRICK-SIMPERS, J.; MEHTA, A. (2018) Accelerated discovery of metallic glasses through iteration of machine learning and high-throughput experiments. **Science Advances**, v. 4, n. 4, p. 1566. Doi:10.1126/sciadv.aaq1566.

ROHLMANN, A.; MOSSNER, U.; BERGMANN, G.; KOLBEL, R. (1982) Finite Element Analysis and experimental investigations of stresses in a femur. **J. Biomed. Eng.**, v. 4, doi:10.1016/0141-5425(82)90009-7

ROYA, R.; MAJUMDARA, A. K. (1981) Thermomagnetic and transport properties of metglas

ISSN: 2236-269X
DOI: 10.14807/ijmp.v11i4.989

2605 SC and 2605. **Journal of Magnetism and Magnetic Materials**, v. 25, n. 1, p. 83–89. Doi:10.1016/0304-8853(81)90150-5.

SCHIRALDI, C.; D'AGOSTINO, A.; OLIVA, A.; FLAMMA, F.; DE ROSA, A.; APICELLA, A.; AVERSA, R.; DE ROSA, M. (2004) Development of hybridmaterials based on hydroxyethylmethacrylate as supports for improving cell adhesion and proliferation. **Biomaterials**, v. 25, n. 17, p. 3645–3653.

SORRENTINO, R. APICELLA, D.; RICCIO, C.; GHERLONE, E. D.; ZARONE, F.; AVERSA, R. E.; GARCIA-GODOY, F. F.; FERRARI, M.; APICELLA, A. (2009) Nonlinear visco-elastic finite element analysis of different porcelain veneers configuration, **Journal of Biomedical Materials Research - Part B Applied Biomaterials**, v. 91, n. 2, p. 727-736; DOI: 10.1002/jbm.b.31449

SORRENTINO, R.; AVERSA, R.; FERRO, V.; AURIEMMA, T.; ZARONE, F.; FERRARI, M.; APICELLA, A. (2007) Three-dimensional finite element analysis of strain and stress distributions in endodontically treated maxillary central incisors restored with different post, core and crown materials. **Dent Mater**, v. 23, p. 983–93: DOI**:** 10.1016/j.dental.2006.08.006

SCHWARTZ-DABNEY, C. L.; DECHOW, P. C. (2003) Variation in Cortical Material Properties Throughout the Human Dentate Mandible. **American Journal of Physical Anthropology**, n. 120, p. 252-277.

TAMAR, G.; HASHIN, Z. V. I. (1980) Analysis of viscoelastic behaviour of bones on the basis of microstructure. **J. Biomechanics**, v. 13, p. 89-96: DOI: http://dx.doi.org/10.1016/0021-9290(80)90182-7

TAYLOR, D.; HAZENBERG, J. G.; LEE, T. C. (2007) Living with cracks: Damage and repair in human bone. **Nat Mater.**, v. 6, p. 263–268.

TÖYRÄSA, J.; LYYRA-LAITINENA, T.; NIINIMÄKIB, M.; LINDGRENC, R.; NIEMINENB, M. T.; KIVIRANTAD, I.; JURVELINA, J. S. (2001) Estimation of the Young's modulus of articular cartilage using an arthroscopic indentation instrument and ultrasonic measurement of tissue thickness. **Journal of Biomechanics**, v. 34, n. 2, p. 251-256

WALKER, R. A.; LOVEJOY, C. O. (1985) Radiographic changes in the clavicle and proximal femur and their use in the determination of skeletal age at death. **Am J Phys Anthropol**, v. 68, p. 67–78.

WANG, W. H.; DONG, C.; SHEK, C. H. (2004) Bulk metallic glasses, **Mater Sci Eng R**, v. 44, p. 45.

WEINANS, H.; HUISKES, R.; GROOTENBOER, H. J. (1992) The behaviour of adaptive bone remodelling simulation models. **J Biomech**., v. 25, p. 1425–1441. PMID: 1491020

WOLFF, J. (1892) Das Gesetz der Transformation der Knochen. **Berlin: A Hirschwald.**